Biochimica et Biophysica Acta 1852 (2015) 839–850

Contents lists available at ScienceDirect

Biochimica et Biophysica Acta

journal homepage: www.elsevier.com/locate/bbadis

Fibroblast growth factor and canonical WNT/β-catenin signaling cooperate in suppression of chondrocyte differentiation in experimental models of FGFR signaling in cartilage

Marcela Buchtova [a,b], Veronika Oralova [b], Anie Aklian [c], Jan Masek [d], Iva Vesela [a], Zhufeng Ouyang [e], Tereza Obadalova [f], Zaneta Konecna [f], Tereza Spoustova [d], Tereza Pospisilova [d], Petr Matula [g], Miroslav Varecha [f], Lukas Balek [d], Iva Gudernova [f], Iva Jelinkova [f], Ivan Duran [h], Iveta Cervenkova [f], Shunichi Murakami [e], Alois Kozubik [d,i], Petr Dvorak [f], Vitezslav Bryja [d,i], Pavel Krejci [d,f,j,*]

[a] Department of Anatomy, Histology and Embryology, University of Veterinary and Pharmaceutical Sciences, Brno, Czech Republic
[b] Institute of Animal Physiology and Genetics AS CR, v.v.i., Brno, Czech Republic
[c] Medical Genetics Institute, Cedars-Sinai Medical Center, Los Angeles, CA, USA
[d] Institute of Experimental Biology, Faculty of Sciences, Masaryk University, Brno, Czech Republic
[e] Department of Orthopaedics, Case Western Reserve University, Cleveland, OH, USA
[f] Department of Biology, Faculty of Medicine, Masaryk University, Brno, Czech Republic
[g] Centre for Biomedical Image Analysis, Faculty of Informatics, Masaryk University, Brno, Czech Republic
[h] Department of Orthopaedic Surgery, David Geffen School of Medicine at UCLA, Los Angeles, CA, USA
[i] Department of Cytokinetics, Institute of Biophysics AS CR, v.v.i., Brno, Czech Republic
[j] International Clinical Research Center, St. Anne's University Hospital, Brno, Czech Republic

ARTICLE INFO

Article history:
Received 15 July 2014
Received in revised form 30 November 2014
Accepted 27 December 2014
Available online 2 January 2015

Keywords:
Fibroblast growth factor receptor
FGFR3
WNT
Chondrocyte
Differentiation
Cartilage

ABSTRACT

Aberrant fibroblast growth factor (FGF) signaling disturbs chondrocyte differentiation in skeletal dysplasia, but the mechanisms underlying this process remain unclear. Recently, FGF was found to activate canonical WNT/β-catenin pathway in chondrocytes via Erk MAP kinase-mediated phosphorylation of WNT co-receptor Lrp6. Here, we explore the cellular consequences of such a signaling interaction. WNT enhanced the FGF-mediated suppression of chondrocyte differentiation in mouse limb bud micromass and limb organ cultures, leading to inhibition of cartilage nodule formation in micromass cultures, and suppression of growth in cultured limbs. Simultaneous activation of the FGF and WNT/β-catenin pathways resulted in loss of chondrocyte extracellular matrix, expression of genes typical for mineralized tissues and alteration of cellular shape. WNT enhanced the FGF-mediated downregulation of chondrocyte proteoglycan and collagen extracellular matrix via inhibition of matrix synthesis and induction of proteinases involved in matrix degradation. Expression of genes regulating RhoA GTPase pathway was induced by FGF in cooperation with WNT, and inhibition of the RhoA signaling rescued the FGF/WNT-mediated changes in chondrocyte cellular shape. Our results suggest that aberrant FGF signaling cooperates with WNT/β-catenin in suppression of chondrocyte differentiation.

1. Introduction

Endochondral ossification, in which bone replaces pre-existing cartilage, is the predominant mechanism of longitudinal bone growth. Bones grow longer at the epiphyseal growth plates, where chondrocytes progress through a series of differentiation stages. Chondrocytes leave their resting state, proliferate in columns, exit the cell cycle and undergo hypertrophy, during which they mineralize their matrix and undergo apoptosis. The cartilage is then replaced by bone [1]. FGF signaling represents one of the major regulators of this process. Removal of FGF-receptor 3 (FGFR3) leads to skeletal overgrowth in mice [2], whereas activating mutations in FGFR3 account for several skeletal dysplasias in humans, e.g., achondroplasia (ACH), which is the most prevalent short-limbed dwarfism, and thanatophoric dysplasia (TD), which represents the most common lethal skeletal dysplasia [3].

One of the hallmark features of FGFR3-related skeletal dysplasia is profound disruption of the growth plate architecture, which, in TD, leads to small or non-existing columns of hypertrophic chondrocytes [4]. This demonstrates the negative effect of aberrant FGF signaling on chondrocyte differentiation, although the mechanisms underlying this phenotype remain unclear. One explanation for this may be FGFR3 interference with indian hedgehog (Ihh)/parathyroid hormone-related

* Corresponding author at: Department of Biology, Faculty of Medicine, Room A3/246, Masaryk University, Kamenice 5, CZ-625 00 Brno, Czech Republic. Tel.: +420 549495395.
E-mail address: krejcip@med.muni.cz (P. Krejci).

http://dx.doi.org/10.1016/j.bbadis.2014.12.020
0925-4439/

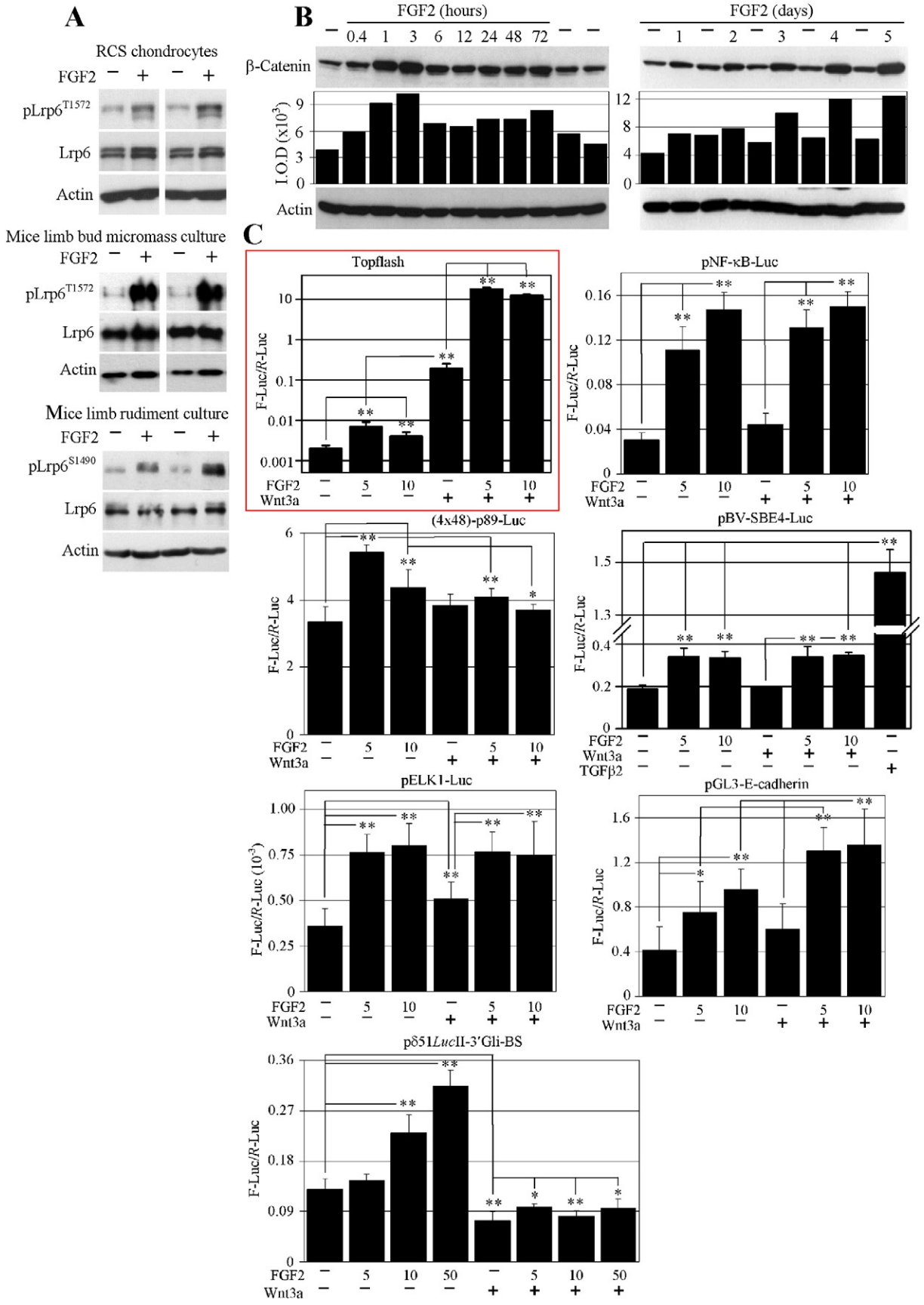
A
RCS chondrocytes
FGF2 − + − +
pLrp6T1572
Lrp6
Actin
Mice limb bud micromass culture
FGF2 − + − +
pLrp6T1572
Lrp6
Actin
Mice limb rudiment culture
FGF2 − + − +
pLrp6S1490
Lrp6
Actin
B
FGF2 (hours)
− 0.4 1 3 6 12 24 48 72 − −
FGF2 (days)
− 1 − 2 − 3 − 4 − 5
β-Catenin
I.O.D (x10³)
Actin
C
Topflash
F-Luc/R-Luc
FGF2 − 5 10 − 5 10
Wnt3a − − − + + +
pNF-κB-Luc
(4x48)-p89-Luc
pBV-SBE4-Luc
TGFβ2
pELK1-Luc
F-Luc/R-Luc (10⁻³)
pGL3-E-cadherin
pδ51LucII-3'Gli-BS
FGF2 − 5 10 50 − 5 10 50
Wnt3a − − − − + + + +

protein (PTHrP) signaling, which is necessary for proper chondrocyte transition from the proliferating to hypertrophic stage [5]. The growth plates of mouse models to both ACH and TD show inhibition of expression of components of Ihh and PTHrP signaling, whereas addition of PTHrP to cultured chondrocytes partially counteracts the cellular phenotypes regulated by FGFR3 [6–9]. In our opinion, impaired Ihh/PTHrP signaling does not account for the full spectrum of chondrocyte differentiation defects observed in TD. Other mechanisms yet to be characterized are likely to mediate the FGFR3 effect on chondrocyte differentiation, hampering our full understanding of the FGFR3 function in bone growth.

Recently, we described the activation of the canonical (i.e., dependent on β-catenin) WNT pathway by FGF signaling in chondrocytes, manifested by FGF-mediated β-catenin stabilization, its increased nuclear accumulation and activation of β-catenin-dependent transcription. This phenotype depends on Erk MAP kinase-mediated phosphorylation of the WNT co-receptor Lrp6 on four conserved intracellular PPPS/TP motifs essential for WNT/β-catenin signal transduction [10,11]. Moreover, FGFR3 mutations associated with skeletal dysplasia exhibit increased signaling via the Erk/Lrp6 pathway [12]. Interestingly, canonical WNT ligands are present in growth plate cartilage, and physiological activation of the WNT/β-catenin pathway promotes chondrocyte differentiation therein, via inhibition of PTHrP signaling and induction of markers typical for terminally differentiated chondrocytes [12–14]. The present study was undertaken to explore the effect of FGF and WNT/β-catenin signaling interaction on regulation of chondrocyte differentiation.

2. Results and discussion

2.1. FGF activates WNT/β-catenin signaling in chondrocytes

Rat chondrosarcoma chondrocytes (RCS) are an immortalized, phenotypically stable cell line that expresses FGFR2 and FGFR3 but not FGFR1 or FGFR4, and produces abundant cartilage-like extracellular matrix (ECM) composed of sulfated proteoglycans and collagen type 2 [15–17]. Activation of FGFR signaling in RCS cells, by addition of exogenous FGF2, resulted in Lrp6 phosphorylation at Ser^{1490} and Thr^{1572} (Fig. 1A) [10] accompanied by β-catenin accumulation persisting for up to 5 days (Fig. 1B). We examined two additional models of cartilage development for FGF2-mediated Lrp6 phosphorylation, i.e., primary cultures of E12 mouse limb bud mesenchymal cells, induced to chondrocyte differentiation via micromass culture [18,19], and limb organ cultures of mouse femurs isolated from E17.5 embryos. Both models responded to FGF2 treatment with Lrp6 phosphorylation (Fig. 1A). Ser^{1490} and Thr^{1572} belong to PPPS/TP motifs on Lrp6 which serve as docking sites that sequester Axin1 and GSK3 from the β-catenin destruction complex, allowing for β-catenin stabilization and transcriptional activation [20]. Removal of PPPS/TP motifs impairs WNT signaling, whereas phosphorylation within the PPPS/TP motifs by kinases independent of the WNT/β-catenin pathway, such as Erk MAP kinase, promotes WNT signaling [21,22]. In RCS chondrocytes, FGF2-mediated Lrp6 phosphorylation enhanced the molecular response to WNT3a (canonical WNT ligand) by more than 100 times [10].

To identify possible effectors underlying the FGF2 and WNT3a signaling interaction, we used multiple luciferase reporters to determine the FGF2 and WNT3a influence on the transcriptional activity of key signaling pathways known to regulate chondrocyte behavior, such as NF-κB, Snail, Elk1 (a reporter for Erk MAP kinase activity), Sox9, Tgfβ and Ihh [11,23–27]. FGF2 and WNT3a modulated the activity of all tested reporters (Fig. 1C). However, these changes were minor compared to the massive β-catenin transcriptional activation (Topflash reporter) induced by FGF2 and WNT3a co-stimulation, suggesting that β-catenin is a major effector of the FGF and WNT signaling interaction.

2.2. FGF2 and WNT3a act in synergy in suppression of chondrocyte differentiation in mouse limb bud micromass cultures and limb organ cultures

Having established that FGF and WNT/β-catenin signaling interact in RCS chondrocytes, we explored the effects of FGF2 and WNT3a treatment on mesenchymal micromass cultures isolated from E12 mouse limb buds. This model recapitulates chondrocyte differentiation *in vitro*, with formation of cartilage nodules observable at 7 days of culture and ECM mineralization detectable at 14 days [28] (Fig. 2A, B). The matrix mineralization observed in the micromass cultures grown for 14 days may have originated from osteoblast differentiation of mesenchymal cells, or from hypertrophic chondrocyte differentiation. As mineralization took place outside but not inside the cartilaginous nodules, it is likely that the mineralized matrix was deposited by newly differentiated osteoblasts rather than hypertrophic chondrocytes (Fig. 2B, right panel). This was confirmed by the quantitative RT-PCR analysis of markers specific to proliferating chondrocytes (*Collagen type 2*), hypertrophic chondrocytes (*Collagen type 10*) and osteoblasts (*Runx2*, *Osteocalcin*), which demonstrated partial decrease of chondrocyte markers at day 14, accompanied by massive upregulation of *Runx2* and *Osteocalcin* messages (Fig. S1).

When used alone, both FGF2 and WNT3a suppressed chondrocyte differentiation in the micromass cultures, as evidenced by a reduction in both the number and size of the chondrocytic nodules developed after 7 days. This phenotype was most pronounced in cells treated simultaneously with both FGF2 and WNT3a (Fig. 2A). In contrast, FGF2 and WNT3a increased matrix mineralization at 14 days of culture, with the strongest effect observed in cultures treated with both growth factors together (Fig. 2B). Thus, FGF appeared to act in synergy with WNT/β-catenin signaling in inhibiting chondrocyte differentiation while enhancing osteoblast differentiation in the micromass cultures (Fig. 2C).

Similar to RCS chondrocytes or limb bud micromass cultures, FGF2 triggered Lrp6 phosphorylation in freshly isolated E17.5 mouse femurs (Fig. 1A). We used limb organ cultures to test whether FGF and WNT/β-catenin signaling cross-talk affected chondrocyte behavior in the growth plate cartilage. Tibias isolated from E18 mouse embryos exhibited normal growth plate architecture, with distinct zones of proliferating and differentiating chondrocytes, including terminally differentiated chondrocytes at the chondro-osseous junction (data not shown). Treatment of such tibias with FGF2 for 8 days resulted in growth plates that were significantly shorter compared to controls and had a markedly disorganized architecture, as manifested by a reduced hypertrophic zone with absence of columnar chondrocytes (Fig. 3A, B). This was confirmed by a reduction of the *Collagen type 10* expression in tibias treated with FGF2 (Fig. 3C). Tibias treated with WNT3a alone grew normally, in contrast to tibias treated with FGF2/WNT3a, which exhibited the most profound growth inhibition accompanied by virtual elimination of *Collagen type 10* expressing chondrocytes.

Fig. 1. FGF2 signaling activates WNT/β-catenin signaling in chondrocytes. (A) RCS chondrocytes, micromass cultures isolated from E12 mouse hindlimb or femurs dissected out from wild-type mouse embryos at E17.5 were treated with FGF2 and analyzed for Lrp6 phosphorylation at Thr^{1572} or Ser^{1490} by WB (pLrp6). Levels of total Lrp6 and actin served as loading controls. (B) RCS chondrocytes were treated with FGF2 (10 ng/ml) for up to 5 days and analyzed for total β-catenin by WB (quantified by densitometry). Note that β-catenin accumulation persisted for the entire duration of the FGF2 treatment. (C) RCS chondrocytes were transfected with the given pathway-specific firefly luciferase reporter (F-Luc) and control *Renilla* luciferase (*R*-Luc) vectors, grown for 24 h, treated with FGF2 (ng/ml) and WNT3a (40 ng/ml) for 20 h and analyzed for luciferase activity. The data represent the average from at least three transfections (each measured twice), with indicated standard deviations. Statistically significant differences are indicated (Student's *t*-test; $^{*}p < 0.05$; $^{**}p < 0.001$). The results are representative of three or four (pGL3-E-cadherin, pTL-ELK1-Luc) experiments. Treatment with TGFβ2 (10 ng/ml) served as a positive control for TGF/BMP (pBV-SBE4-Luc reporter) signaling activation. Note the strong Topflash activation (red square) mediated by FGF2/WNT3a (logarithmic scale for the *y*-axis) compared to the rather minor changes in the activities of other reporters.

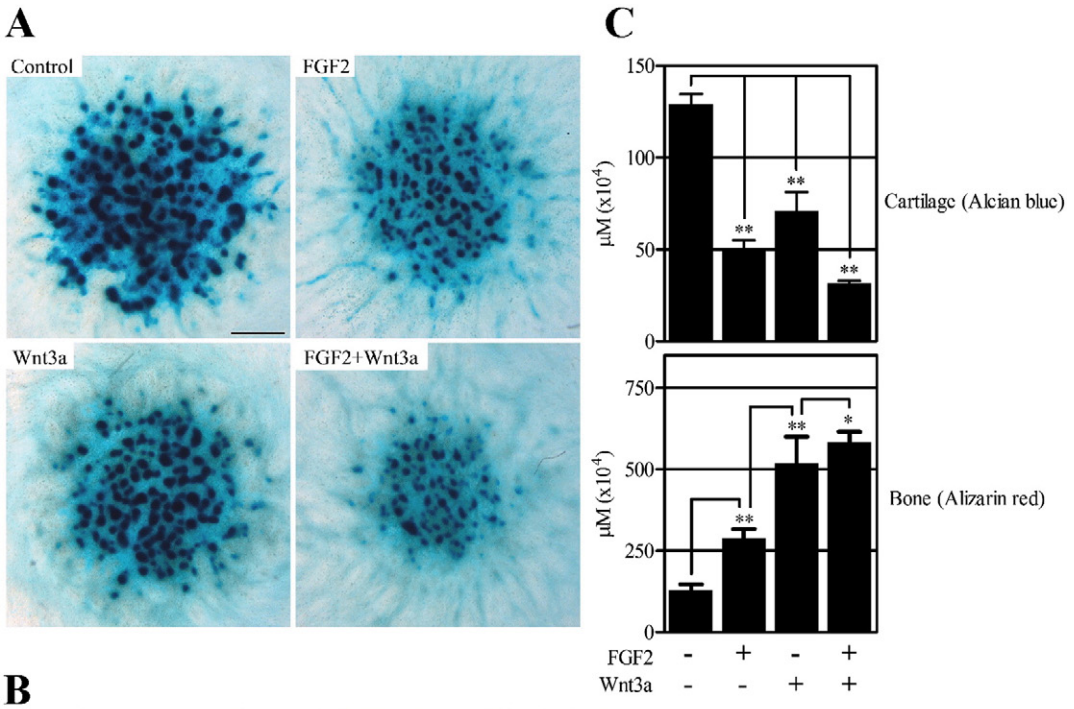
A
Control
FGF2
Wnt3a
FGF2+Wnt3a
C
150
100
50
0
μM (x10⁴)
**
**
**
Cartilage (Alcian blue)
750
500
250
0
μM (x10⁴)
**
**
*
Bone (Alizarin red)
FGF2 - + - +
Wnt3a - - + +

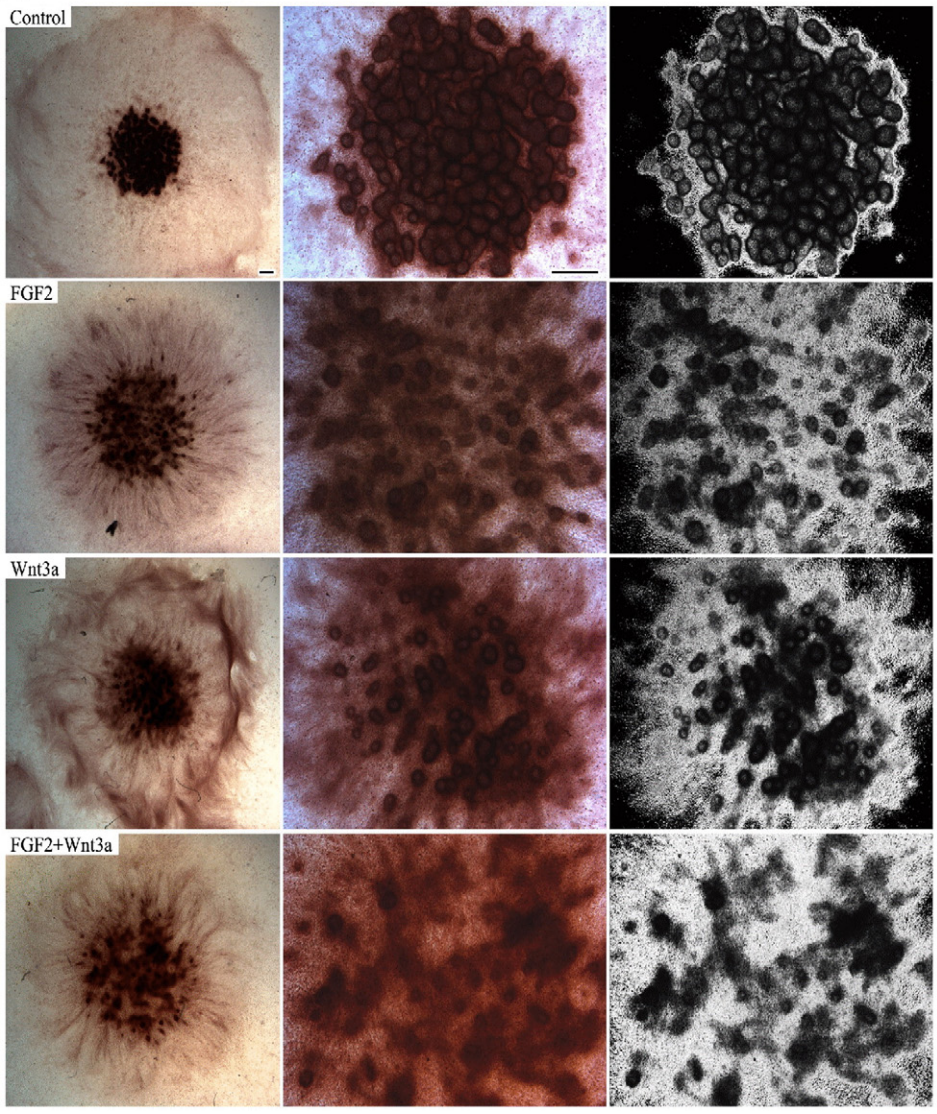
B
Control
FGF2
Wnt3a
FGF2+Wnt3a

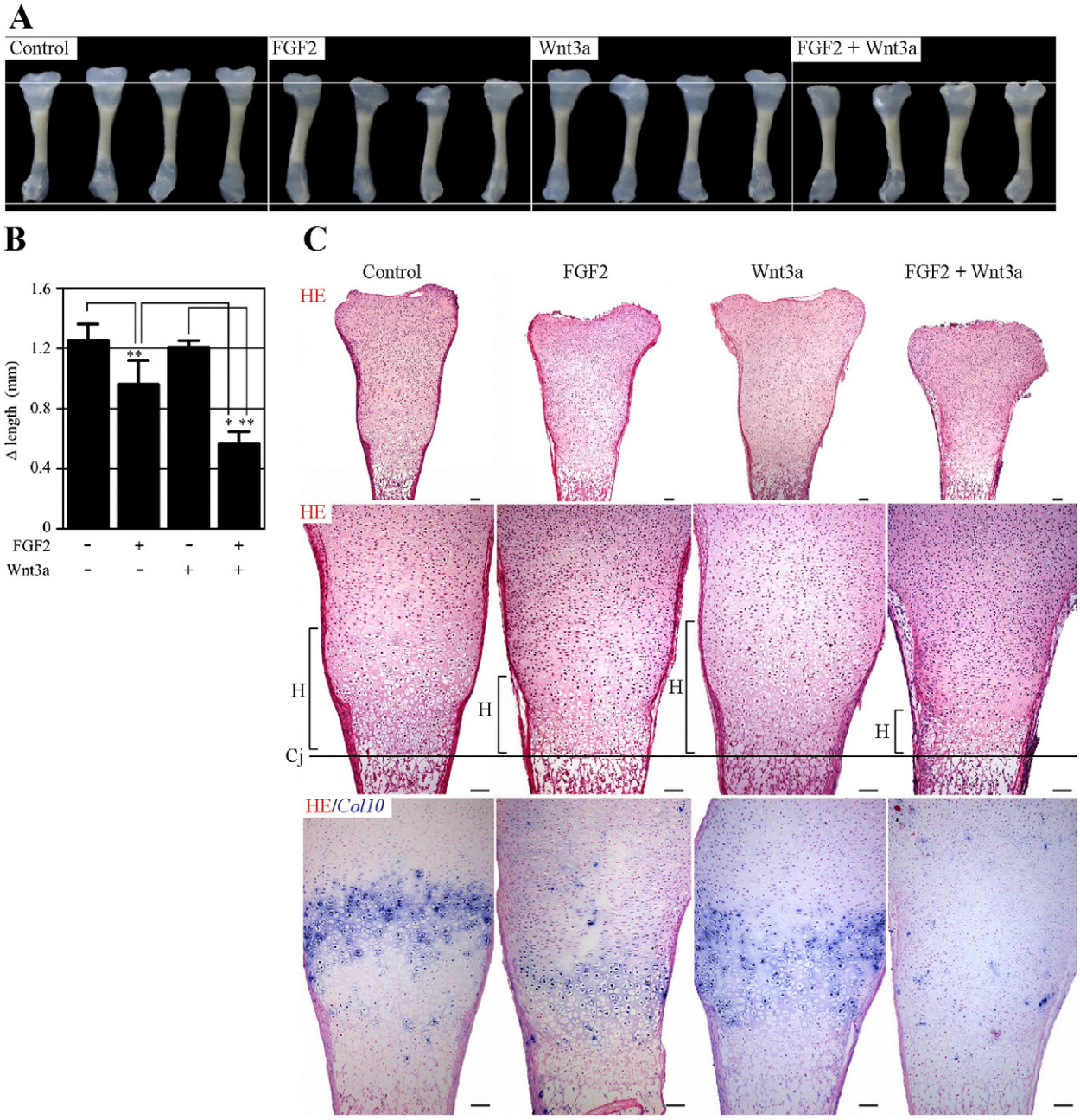

Fig. 3. FGF2 and WNT3a inhibit growth in mouse limb organ culture. (A) Mouse tibias isolated from E18 embryos were cultured in media supplemented by FGF2 (50 ng/ml) and/or WNT3a (40 ng/ml) for 8 days. Four biological replicates are shown for each treatment. The length of each tibia was measured after the extraction from the embryo and after 8 days of incubation. The graph shows differences between both time points (Δ length) (B). Statistically significant differences are highlighted (ANOVA, $^{*}p < 0.05$; $^{**}p < 0.001$). Note that FGF2-mediated growth inhibition was potentiated by WNT3a. The results are representative of three independent experiments. (C) Histological sections of representative tibias were stained with hematoxylin/eosin (HE). Note the marked reduction of hypertrophic cartilage (H) in tibias treated with FGF2 and FGF2/WNT3a, with corresponding loss of *Collagen type 10* expression (bottom panel, *Collagen type 10* in situ hybridization counterstained with eosin). Cj, chondro-osseous junction.

No similar effect on FGF2-mediated growth inhibition was found in tibias treated by non-canonical (i.e., β-catenin independent) WNT ligand WNT5a (Fig. S2). This demonstrates, along with the published literature [29], that FGF signaling interferes with hypertrophic chondrocyte differentiation in the growth plate. Activation of the WNT/β-catenin pathway by treatment with WNT3a augmented this effect.

2.3. FGF2 and WNT3a cooperate in regulation of chondrocyte cellular shape and ECM turnover

In RCS chondrocytes, FGFR activation leads to rapid loss of chondrocyte sulfated proteoglycan ECM via inhibition of matrix synthesis and active proteolytic degradation [30,31]. As evidenced by alcian blue

Fig. 2. FGF2 and WNT3a alter chondrocyte differentiation in mouse limb micromass cultures. (A) Alcian blue staining of mouse hindlimb micromass culture treated with FGF2 (10 ng/ml) and/or WNT3a (10 ng/ml) for 7 days. (B) Alizarin red staining of micromass grown for 14 days. The white area in the right panel represents the signal used for quantification. Bar — 500 μm. (C) Graphs showing levels of alcian blue staining of the cartilage matrix (A) or alizarin red staining of the calcified matrix (B). The data represent the average ± standard deviation of four independent biological replicates. Statistically significant differences are highlighted (ANOVA, $^{*}p < 0.05$; $^{**}p < 0.001$). The results are representative of three independent experiments. Note the decrease in amounts and size of cartilage nodules in FGF2 and WNT3a treated cultures, with the strongest effect in cultures treated with FGF2/WNT3a. Also note the positive effect of both FGF2 and WNT3a on the matrix mineralization, which was most pronounced in cultures treated with FGF2/WNT3a.

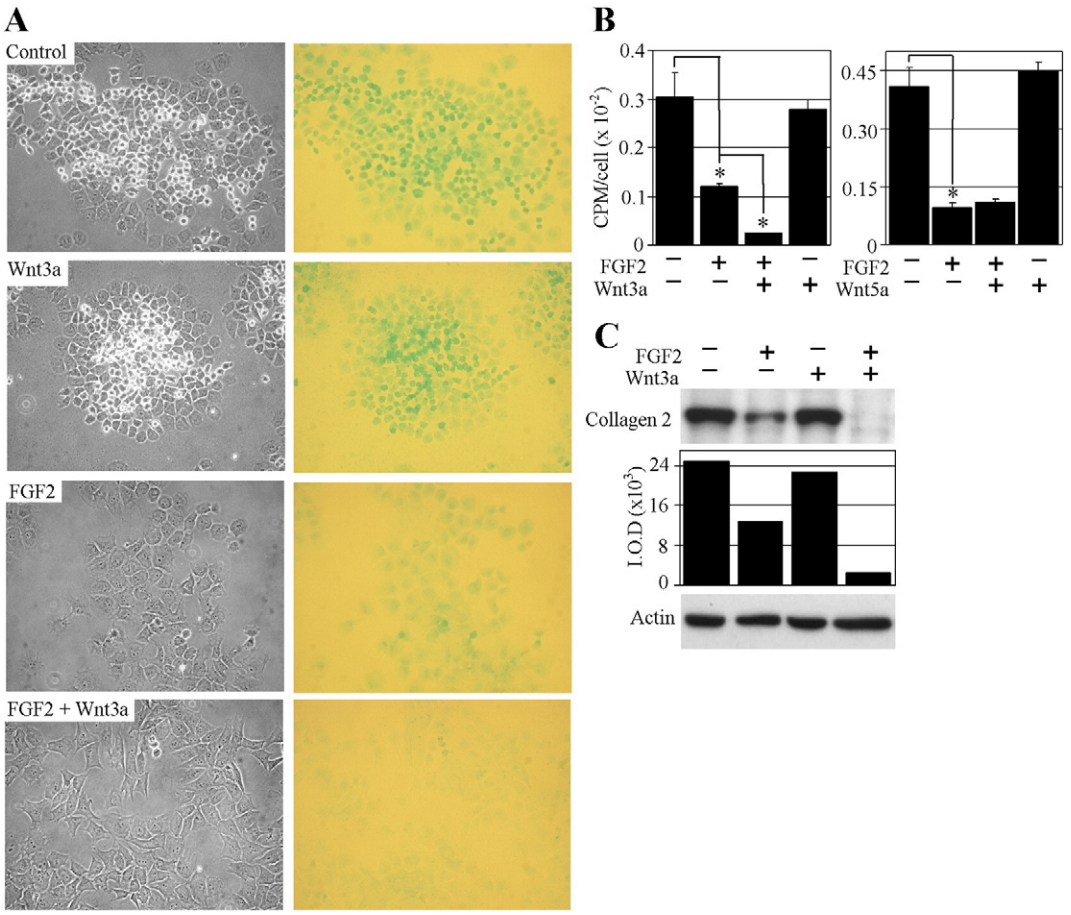

Fig. 4. FGF2 and WNT3a suppress ECM production in RCS chondrocytes. (A) Cells were treated with FGF2 (10 ng/ml) and WNT3a (50 ng/ml), stained with alcian blue to visualize the sulfated proteoglycan ECM and photographed (dark field with contrast, 200x). (B) To quantify matrix production, cells were treated with FGF2 (10 ng/ml) and WNT3a (50 ng/ml) in the presence of [^{35}S]sulfate for 72 h and the amount of incorporated radioactivity was determined by liquid scintillation. The data represent the average from four wells, with the indicated standard deviations (Student's *t*-test; $^{*}p < 0.001$). Treatment with non-canonical WNT5a (50 ng/ml) served as a negative control. (C) RCS chondrocytes were treated with FGF2 (10 ng/ml) and WNT3a (40 ng/ml) for 48 h and analyzed for collagen type 2 expression by WB. Note the negative FGF2-mediated effect on collagen type 2 quantity, which was further downregulated by concomitant WNT3a treatment (quantified by densitometry). Actin served as loading control.

staining, this phenotype was strongest in cells treated with FGF2/WNT3a; WNT3a alone did not alter ECM production (Fig. 4A). This was confirmed by metabolic proteoglycan labeling with [^{35}S]sulfate used to quantify the amounts of sulfated proteoglycan ECM [30] (Fig. 4B). Apart from proteoglycan ECM, the production of collagen ECM was also downregulated by FGF signaling, as evidenced by decreased expression of collagen type 2 following FGF2 treatment; this effect was enhanced by WNT3a, resulting in a lack of detectable collagen type 2 expression in cells treated with FGF2/WNT3a for 72 h (Fig. 4C).

Alteration of chondrocyte cellular shape is a key histological feature of FGFR3-related skeletal dysplasia [4]. In RCS chondrocytes, a similar phenotype was manifested as cell enlargement and flattening following treatment with FGF2, accompanied by cytoskeletal remodeling, illustrated here by phalloidin staining of the actin stress fibers (Fig. 5A, D). A subjective increase in substrate adhesion was also observed in chondrocytes treated with FGF2, shown by vinculin staining of focal adhesions (Fig. 5C). Although WNT3a had no effect on RCS cellular shape when used alone, it enhanced the changes mediated by FGF2, i.e., caused elongation along a single axis when compared to cells treated with FGF2 alone, which spread uniformly in all directions (Fig. 5A) (Supplementary movie 1). We quantified these changes by measuring the cell perimeter, which increases with cell size and complexity of the cell boundary. The data presented in Fig. 5B demonstrates ~1 fold perimeter increase in cells treated with FGF2 and FGF2/WNT3a when compared to untreated cells. Differences in cell shape were quantified by determining the extend of cell "eccentricity", reflecting elongation along one axis. FGF2 increased cell eccentricity and this phenotype was significantly enhanced by WNT3a, while no changes in cell shape were found in cells treated with WNT3 alone or in cells treated with WNT5a alone or in combination with FGF2 (data not shown).

To identify genes involved in cellular phenotypes regulated by FGF2 and WNT3a, we carried out expression profiling in RCS chondrocytes treated with FGF2 and/or WNT3a for 16 or 48 h, taking into account that FGF2/WNT3a-mediated changes on ECM and cellular shape required at least 48 h to fully manifest [30] (Supplementary movie 1). Gene expression profiling showed that WNT3a enhanced the FGF2 inhibitory effect on expression of several key components of the ECM (*Collagen type 2, Collagen type 9*, *Aggrecan*, *Chondroitin sulfate proteoglycan 4, Cartilage immediate layer protein, Chondroadherin*), as well as proteins involved in proteoglycan production, such as *chondroitin sulfate synthase 3* (Table 1). In addition, WNT3a enhanced the FGF2-mediated induction of several enzymes involved in ECM catabolism, such as heparanase and several proteinases belonging to the *Adamts* (*A disintegrin and metalloproteinase with thrombospondin motifs*) family. Although FGF2 increased expression of *Adamts4* and *Adamts5*, which are the main proteinases responsible for aggrecan degradation *in vivo* [32], WNT3a appeared to inhibit

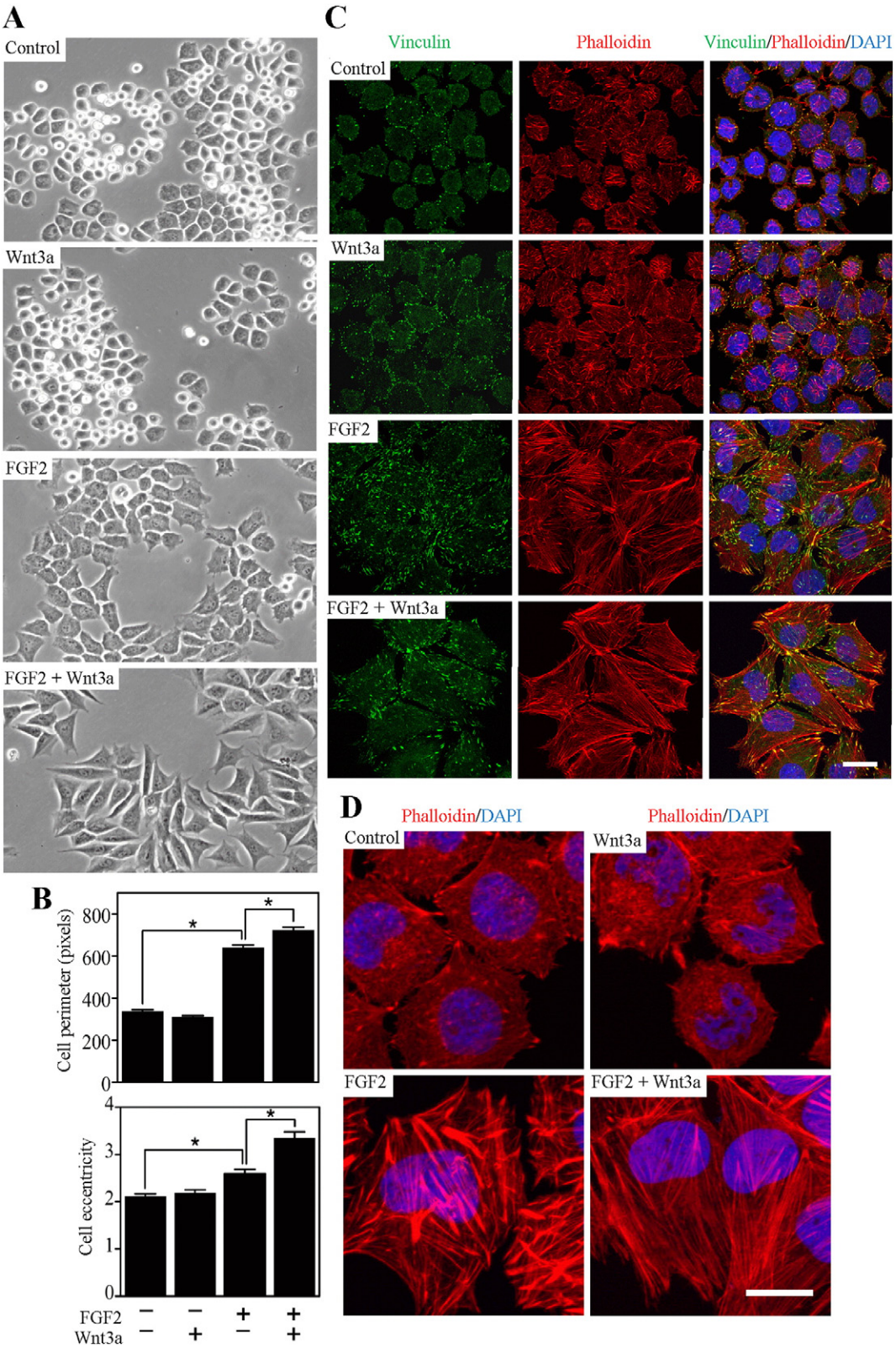

Fig. 5. FGF2 and WNT3a alter cellular shape in RCS chondrocytes. (A) RCS chondrocytes were treated as indicated for 72 h and photographed (dark field with contrast, 200x), or stained for DNA (DAPI), focal adhesions (vinculin) and actin stress fibers (phalloidin) and analyzed by immunocytochemistry (bars, 25 μm) (C, D). (B) Changes in cellular shape were quantified by determining the cell perimeter and eccentricity (equal to 1 for perfect disc-like cells and >1 for elongated cells). The data represent measurements of 345 cells in each treatment with indicated standard errors. Statistical differences are highlighted (ANOVA, $^{*}p < 0.001$). Note the FGF2 effect on overall cell shape and actin stress fiber formation, which was further enhanced by WNT3a, with elongation along a single axis observable in some cells.

rather than increase this effect (Table 1). Other proteinases may therefore be responsible for the synergistic effect of FGF2 and WNT3a on proteoglycan ECM degradation in chondrocytes (Fig. 4). Interestingly, WNT3a significantly enhanced the FGF2-mediated induction of expression of *Adamts1*, *Adamts6* and *Adamts7*, which are all capable of degrading aggrecan [33,34].

Table 1
Extracellular matrix, cytoskeletal, differentiation and Rho pathway-related genes regulated by FGF2 and WNT3a signaling in RCS chondrocytes. Cells were treated with FGF2 (F; 10 ng/ml) and WNT3a (W; 40 ng/ml) for 16 and 48 h and then expression profiling was carried out. The data represent the fold difference compared to untreated controls. Underlined data indicate when WNT3a enhanced the FGF2 effect on the given gene expression by more than one fold (100%) relative to the control. X, confirmation of gene expression by real-time RT-PCR (qPCR). *Cspg4*, chondroitin sulfate proteoglycan 4; *Cilp*, cartilage intermediate layer protein; *Chsys3*, chondroitin sulfate synthase 3; *Ctgf*, connective tissue growth factor; *Lim1*, actin binding Lim protein 1; *Grinl1a*, Grinl1a combined protein; *B2F*, B2F high sulfur protein; *Ahrgap18*, Rho GTPase activating protein 18; *Srgap*, Slit-Robo GTPase-activating protein; *Fgd*, FYVE, RhoGEFand PH domain containing 3. The value is underlined when a given gene is expressed by more than one fold (100%) relative to the control.

Gene	Accession no.	Function	F16	W16	FW16	F48	W48	FW48	qPCR
Aggrecan	NM_022190	Extracellular matrix component	−1.32	−1.07	−2.07	−1.62	−1.13	−11.5	X
Cspg4	NM_031022	Extracellular matrix component	−6.32	−1.05	−8.30	−7.77	−1.07	−12.9	X
Lumican	NM_031050	Extracellular matrix component	1.40	−2.12	2.27	4.58	−2.70	10.61	X
Chondroadherin	NM_019164	Extracellular matrix component	1.00	−1.19	1.05	−2.34	−1.42	−4.00	X
Cilp	NM_001108161	Extracellular matrix component	−1.89	−1.65	−2.70	−2.26	−1.17	−7.15	X
Collagen 2a1	NM_012929	Extracellular matrix component	−1.43	−1.20	−2.54	−2.14	−1.15	−7.88	X
Collagen 5a2	NM_053488	Extracellular matrix component	10.71	−1.38	9.65	13.92	−1.24	12.95	
Collagen 9a2	NM_001108675	Extracellular matrix component	−1.37	−1.07	−1.84	−2.03	−1.07	−4.37	X
Chsys3	XM_225912	Proteoglycan synthesis	−3.30	−1.33	−5.22	−2.40	−1.22	−3.01	X
Heparanase	NM_022605	Extracellular matrix degradation	4.55	1.09	5.98	3.66	1.07	3.44	X
Adamts1	NM_024400	Extracellular matrix degradation	1.84	−1.44	6.60	3.41	−1.34	6.22	X
Adamts4	NM_023959	Extracellular matrix degradation	2.62	−1.73	1.83	4.30	−1.95	1.56	
Adamts5	NM_198761	Extracellular matrix degradation	3.98	−1.19	3.20	4.55	1.26	2.07	
Adamts6	NM_001108544	Extracellular matrix degradation	3.15	−1.28	3.78	2.63	−1.37	4.14	X
Adamts7	NM_001047101	Extracellular matrix degradation	2.28	−1.19	3.21	2.47	−1.11	4.96	X
Ctgf	NM_022266	Osteoinductive growth factor	5.08	2.75	7.76	4.70	3.44	4.99	X
Osteoglycin	NM_001106103	Osteoinductive growth factor	3.15	1.71	3.30	5.12	5.08	10.51	
Osteoactivin	NM_133298	Osteoblast differentiation	6.49	1.32	6.37	4.89	1.59	5.31	
S100a4	NM_012618	Calcium ion binding	27.13	−1.84	33.97	18.72	−1.05	36.67	X
Lim1	NM_001044394	Actin binding protein	3.24	−1.00	4.92	6.05	−1.11	29.42	X
Drebrin1	NM_031024	Actin binding protein	1.97	1.30	2.56	2.91	1.26	4.19	X
Grinl1a	NM_001014211	Cytoskeletal structure	1.37	1.69	46.18	1.18	4.45	40.52	
Keratin33b	NM_001008819	Cytoskeletal structure	1.14	1.09	13.35	−1.27	3.84	6.33	X
Keratin39	NM_001004130	Cytoskeletal structure	12.09	1.59	127.0	8.88	1.65	43.16	
B2F	NM_001025135	Cytoskeletal structure	36.91	6.47	125.3	51.23	13.11	75.05	
Protocadherin18	NM_001100524	Cell adhesion molecule	2.00	1.06	4.60	5.35	1.32	6.62	X
Protocadherin β19	XM_001056051	Cell adhesion molecule	4.99	−1.90	5.19	5.35	−1.34	13.52	
Protocadherin β21	NM_001114604	Cell adhesion molecule	4.37	1.17	4.20	5.70	1.07	8.38	X
Cadherin19	NM_001009448	Cell adhesion molecule	−1.27	−3.33	−4.48	−1.28	−3.22	−4.49	X
Integrin α4	NM_001107737	Cell adhesion molecule	1.36	1.07	4.99	5.08	1.76	28.68	X
Integrin α7	NM_030842	Cell adhesion molecule	2.52	1.20	3.25	1.74	1.15	4.14	X
Osteomodulin	NM_031817	Cell adhesion molecule	45.40	29.0	216.3	46.74	96.30	715.6	
Cdc42gap	NM_001105879	Cdc42 inhibitor	−3.14	−1.07	−3.25	−2.82	−1.12	−4.13	X
Ahrgap18	NM_001106354	Rho inhibitor	1.50	−1.26	2.02	2.56	−1.16	3.02	
Srgap1	NM_001191784	Rho inhibitor	1.59	1.64	3.08	1.49	2.31	2.91	X
Srgap3	NM_001191975	Rho inhibitor	2.85	−1.34	9.41	3.78	−1.47	5.95	X
Fgd3	NM_001108409	Rho activator	2.71	−1.10	2.73	2.12	1.27	3.08	
Fgd6	NM_001137645	Rho activator	3.43	1.00	4.77	2.23	1.03	3.42	X
RhoE	NM_001007641	Small GTPase	2.17	−1.01	3.63	2.55	1.25	4.45	X

FGF2 and WNT3a also acted synergistically in regulation of RCS cellular morphology (Fig. 5). FGF2 and WNT3a enhanced expression of several genes involved in cytoskeletal remodeling (*Actin binding LIM protein1, Drebrin1*), structural components of the cytoskeleton (*GRINL1A combined protein*, members of the *Keratin* family, *High sulfur protein B2F*) and cell adhesion molecules (*Integrin α4*, *Integrin α7*, *Cadherin 19*, members of the *Protocadherin* family) (Table 1). Importantly, FGF2 and WNT3a also modulated expression of six genes encoding proteins participating in signaling of the Rho family of GTPases. These included RhoA inhibitors *Arhgap18*, *Srgap1*, *Srgap3*, RhoA activators *Fgd3* and *Fgd6*, and *RhoE* GTPase [35–38]. RhoA, Rac1 and Cdc2 are prototype members of Rho family GTPases that mediate cytoskeletal remodeling during cell adhesion, changes in cell morphology and cell migration. Although all three proteins regulate the actin cytoskeleton, they differ in the nature of the regulated process. While Cdc42 and Rac1 induce lamellipodia and filopodia necessary for cell migration, RhoA activation regulates formation of actin stress fibers and subsequent changes in cell morphology [39]. We did not observe increased migration nor formation of lamellipodia and/or filopodia in chondrocytes treated with FGF2 and/or WNT3a (Supplementary Movie 1), suggesting that Cdc42 and Rac1 do not participate in changes of RCS chondrocyte morphology mediated by FGF2. RhoA is required for formation of focal adhesions, where components of ECM, such as fibronectin, interact, via integrins, with the actin cytoskeleton [40,41]. Interestingly, FGF2 and WNT3a appeared to increase the amount of RCS focal cell adhesions, although we did not precisely quantify this phenotype (Fig. 5C). We previously reported a potent increase in fibronectin production induced by FGF2 of RCS chondrocytes [30].

Overall, the formation of actin stress fibers, changes in cell morphology and absence of lamellipodia or filopodia formation point toward RhoA as the predominant Rho GTPase modulated by FGF and WNT/β-catenin signaling in RCS chondrocytes. We tested this hypothesis by evaluating the effect of chemical inhibition of the RhoA pathway on the cellular shape changes mediated by FGF2 and WNT3a treatments.

Fig. 6. Inhibition of the Rho pathway rescues the FGF2/WNT3a-mediated changes in RCS chondrocyte cellular shape. (A) Cells were treated with FGF2 (5 ng/ml) and/or WNT3a (40 ng/ml) in the presence of RhoA pathway inhibitors HA1100 (70 μM) and Y27632 (20 μM), and analyzed for cell shape changes 72 h later (dark field with contrast, 200x). Both p160ROCK inhibitors rescued the FGF2/WNT3a-mediated changes in cell shape, with no effect observed in untreated cells or cells treated with WNT3a alone. (B) RCS chondrocytes were transfected with the RhoA-DN-GFP vector, then treated with FGF2 (10 ng/ml) and WNT3a (40 ng/ml) for 72 h. Expression of the dominant-negative RhoA variant rescued the FGF2/WNT3a effect on RCS cellular shape (GFP-positive cells), in contrast to non-transfected cells (DIC, differential contrast; DAPI, nuclear staining; Bar, 50 μm).

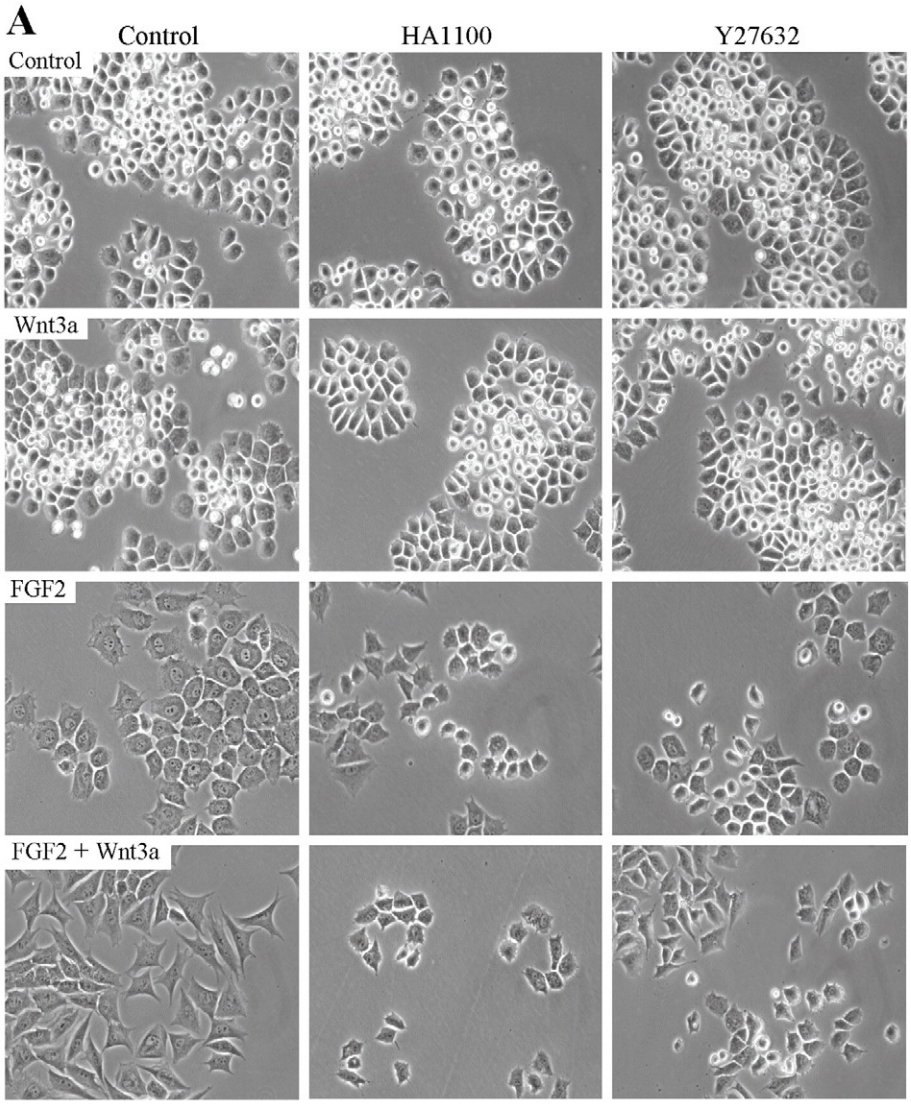
A
Control
HA1100
Y27632
Control
Wnt3a
FGF2
FGF2 + Wnt3a

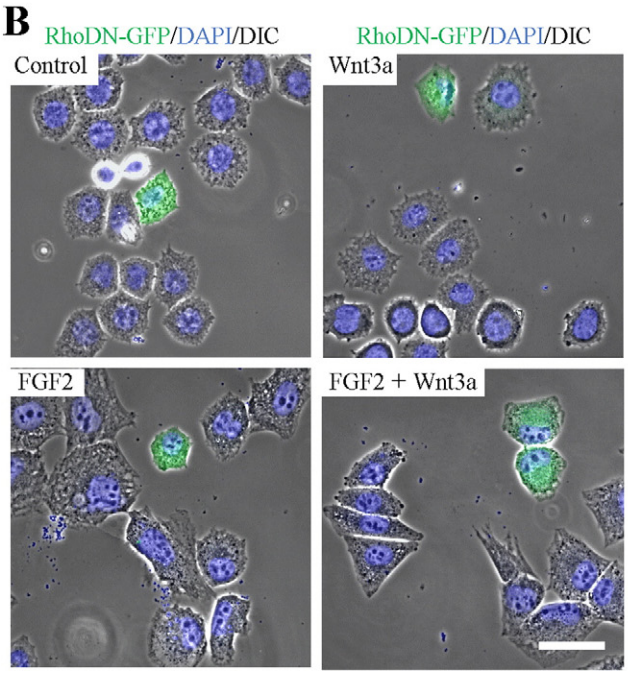
B
RhoDN-GFP/DAPI/DIC
RhoDN-GFP/DAPI/DIC
Control
Wnt3a
FGF2
FGF2 + Wnt3a

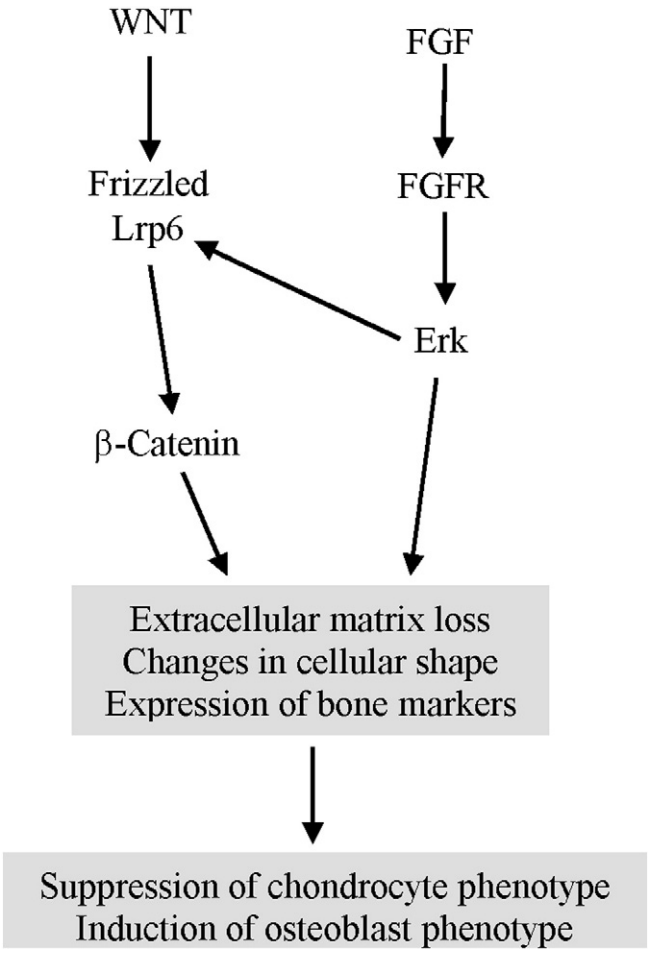

Fig. 7. Model of the FGF and WNT/β-catenin signaling interaction. Activation of FGF signaling promotes WNT/β-catenin signaling in chondrocytes via Erk MAP kinase-mediated phosphorylation of WNT co-receptor Lrp6 on intracellular PPPS/TP motifs essential for WNT/β-catenin signal transduction. The FGF and WNT/β-catenin pathways act in synergy in regulation of gene transcription, leading to loss of extracellular matrix, changes in cellular shape and expression of genes typical for mineralized tissues. Together, these changes underlie changes in cell differentiation status, manifested as suppression of the chondrocyte phenotype and partial induction of the osteoblast phenotype.

The major RhoA signaling intermediate, p160ROCK kinase, was inhibited by two unrelated chemical inhibitors, i.e., HA1100 and Y27632 [42,43]. Both compounds rescued the RCS cellular shape change induced by FGF2/WNT3a. No observable effect on cellular shape or proliferation was found for either drug in FGF2-naïve cells (Fig. 6A). In addition, transfection with dominant-negative (T19N) RhoA mutant, C-terminally tagged with GFP did not significantly alter the cellular shape in control or WNT3a-treated cells but did rescue both the FGF2 and FGF2/WNT3a-mediated changes of RCS cellular shape (Figs. 6B, S3).

2.4. FGF2 and WNT3a alter chondrocyte differentiation status

Compared to most tissues of mesenchymal origin, FGF signaling triggers paradoxical changes in cartilage. It is clear that major cell phenotypes defining the molecular pathology of FGFR3-related skeletal dysplasia (i.e., chondrocyte growth arrest, loss of ECM and disturbed differentiation) constitute only part of rather complex changes in chondrocyte behavior induced by FGF signaling. Under chronic FGFR activation, chondrocytes begin to lose their differentiated status, characterized by high production of sulfated proteoglycans and collagen type 2. At the same time, mesenchymal markers, such as collagen type 1 and 5, fibronectin, α-smooth muscle actin and S100a4, appear together with altered cell morphology resembling undifferentiated mesenchymal cells. Expression of genes typical for mineralized tissues (*Collagen type 3*, *Ctgf*, *Osteomodulin*, *Osteonectin*, *Osteocalcin*, *Osteoglycin*, *Osteoactivin*) increases in RCS chondrocytes and several other *in vitro* and *in vivo* chondrocyte models (Table 1) [16,30,44–52]. Collectively, this evidence suggests that FGF signaling suppresses chondrocyte differentiation status, while at the same time forcing the cells to express an osteoblast-like phenotype (Fig. 7).

It is unclear whether the abovementioned changes originate entirely from a direct transcriptional response to FGFR3 activation or there are other pathways involved in the process. In this respect, activation of the RhoA pathway by FGF2 and FGF2/WNT3a might serve other roles besides actin cytoskeletal reorganization (Fig. 5). Activation of RhoA accompanies chondrocyte de-differentiation in vitro, whereas mesenchymal cells grown in alginate gel or limb micromass culture lose RhoA expression during their chondrocytic differentiation. In addition, chemical inhibition of the Rho pathway restores expression of cartilage genes via upregulation of Sox9 activity, and RhoA overexpression in ATDC5 cells delays their differentiation into hypertrophic chondrocytes [53,54]. Consistent with these findings, the FGF2/WNT3a-mediated suppression of hypertrophic chondrocyte differentiation observed in all three chondrocyte models used here suggests active involvement of RhoA in this process (Figs. 2-5). Experiments are ongoing to test this hypothesis.

Similar to FGF, canonical WNT/β-catenin signaling regulates several essential physiological processes in skeletogenesis. First, it promotes osteoblast cell fate at the expense of chondrocyte cell fate in differentiating mesenchymal osteo-chondroprogenitors [55]. Second, it accelerates terminal hypertrophic differentiation in the mature chondrocytes of growth plate cartilage via inhibition of the PTHrP signaling necessary for maintenance of proliferation, inhibition of *Sox9* and *Collagen type 2* transcription and induction of *Matrix metalloproteinase (mmp) 13*, *Adamts5*, *Collagen type 10*, *Runx2* and *Alkaline phosphatase* [13,14,56]. Ectopic activation of WNT/β-catenin signaling in murine growth plate cartilage results in neonatal lethal dwarfism characterized by a flattened skull and markedly shortened and hypoplastic long bones [57]. Limb histology revealed the virtual absence of typical growth plate architecture, instead consisting of undifferentiated chondrocytes with altered cell morphology and poor expression of aggrecan, collagen type 2 and 9, and Sox9. Similarly, isolated chick sternal chondrocytes overexpressing constitutively active β-catenin adopted a fibroblastic and flat-shaped morphology, accompanied by downregulation of proteoglycan ECM via induction of Adamts5 and Mmp2, 3, 7 and 9 [57]. As many of the latter phenotypes resemble typical features of FGFR3-related skeletal dysplasia, the evidence presented in this article allows for speculation that activation of WNT/β-catenin contributes to the effects of aberrant FGF signaling in cartilage.

3. Materials and methods

3.1. Cell, micromass and limb organ cultures

Cells were propagated in DMEM media supplemented with 10% FBS and antibiotics (Invitrogen, Carlsbad, CA). For growth assays, 1×10^4 cells were grown in 24-well tissue culture plates for 72 h and counted. The growth factors and chemicals were obtained from the following manufacturers: FGF2, WNT3a, WNT5a (R&D Systems, Minneapolis, MN); TGFβ2 (Sigma-Aldrich, St. Louis, MO); HA1100, Y27632 (Tocris Bioscience, Ellisville, MO). Femurs were dissected out from wild-type mouse embryos at E17.5, and cultured in α-MEM media (Invitrogen) supplemented with 0.2% BSA. All animal experiments were reviewed and approved by the Institutional Animal Care and Use Committee at Case Western Reserve University (protocol number 2010-0023). To ameliorate suffering, mice were euthanized by CO_2 inhalation in accordance

with AVMA Guidelines on Euthanasia. Tibias were dissected out from mouse embryos at E18, placed on Millipore filters above a metal mesh and cultured in differentiating media (60% F12/40% DMEM, 10% FBS, 50 μg/ml ascorbic acid, 10 mM β-glycerol phosphate) for 8 days at 37 °C. Primary mesenchymal cultures were established from the hindlimb bud of E12 mouse embryos. Proteolytic digestion was performed using dispase II (10 U/ml; Sigma), followed by filtration of the cell suspension through a cell strainer to obtain a single-cell population. 2×10^7 cells/ml were plated in 10 μl aliquots and left to adhere for 1 h before differentiating media was added.

3.2. Western blotting (WB) and immunocytochemistry

Cells were lysed in buffer containing 50 mM Tris–HCl pH 7.4, 150 mM NaCl, 0.5% NP-40, 1 mM EDTA and 25 mM NaF supplemented with proteinase inhibitors. The femurs were cleaned of the soft tissues under the preparation microscope, the growth plate cartilages were separated from bone, and used for Western blotting. Protein samples were resolved by SDS-PAGE, transferred onto a PVDF membrane and visualized by chemiluminiscence (Thermo Scientific, Rockford, IL). Integrated optical density (I.O.D.) of the WB signal was quantified by Scion Image software (Scion Corporation, Frederick, MA). The following antibodies were used: β-catenin (BD Biosciences, Rockville, MD); Lrp6, pLrp6^{S1490} (Cell Signaling, Beverly, MA); pLrp6^{T1572} (Millipore, Billerica, MA); actin (Santa Cruz Biotechnology, Santa Cruz, CA); collagen type 2 (Cedarlane Laboratories, Ontario, Canada). For immunocytochemistry, cells were fixed in 4% paraformaldehyde, stained with vinculin-FITC (Sigma-Aldrich) antibody according to the manufacturer's protocol and mounted in Vectashield medium containing DAPI (Vector Laboratories, Burlingame, CA). Polymerized actin was visualized using AlexaFluor 594-conjugated Phalloidin (Life Technologies, Grand Island, NY).

3.3. Time-lapse and confocal microscopy, image analysis

Confocal fluorescence and two photon laser scanned images were captured on a Leica TCS-SP MP confocal microscope (Heidelberg, Germany). Time-lapse microscopy of RCS cultures was conducted using BioStation CT microscope (Nikon, Japan). Phase contrast images of several cell samples were automatically acquired every 15 min for 72 h. Images were processed using VirtualDub (www.virtualdub.org) software to increase overall contrast and sharpness, and remove image shaking. For cellular shape analyses, 345 cells were outlined in each treatment group and their areas were manually filled by an unbiased scientist. The cell shape was quantified by computing two parameters, namely perimeter and eccentricity, using the DIPimage toolbox (TU Delft, the Netherlands). The perimeter was calculated by a chain-code method. The eccentricity was calculated as the ratio of moments of inertia of the cellular area.

3.4. Cell transfection, luciferase reporter assays, expression profiling and real-time

RT-PCR cells were transfected using FuGENE6 according to the manufacturer's protocol (Roche, Indianopolis, IN). For the luciferase reporter assays, the μg ratio between the Firefly luciferase vector and pRL-TK (Promega, Madison, WI) control vector was 3:1. The luciferase activity was determined using a dual-luciferase reporter assay (Promega). The following vectors were used: pELK1-Luc (Panomics, Fremont, CA), pBV-SBE4-Luc [58], pGL3-E-cadherin [59], (4x48)-p89-Luc [60], pδ51*Luc*II-3′Gli-BS [61], pNF-κB-Luc (Agilent Technologie, Santa Clara, CA) and Topflash (obtained from R. Moon). The vector expressing dominant-negative RhoA (pcDNA3-EGFP-RhoA-T19N) was obtained from Addgene (Cambridge, MA). For microarray analysis, total RNA was isolated using the RNeasy mini kit and cleaned with a RNeasy spin column (Qiagen, Valencia, CA). All reagents and equipment used for the subsequent analyses were from Affymetrix (Santa Clara, CA). cDNA was synthesized using the GeneChip WT cDNA synthesis kit and random hexamers tagged with a T7 promoter sequence. Single-stranded cDNA was hybridized to probe sets present on a GeneChip rat gene 1.0 ST array, offering whole genome transcript coverage. Two to three independent biological samples were analyzed for each treatment and the control. The intensity files were produced using GeneChip Operating Software v1.4 and analyzed with Expression Console software v1.1. using the PLIER algorithm. For real-time RT-PCR, total RNA was isolated using the RNeasy mini kit (Qiagen) and poly-dT-primed cDNA was synthesized from 3 μg of RNA using a Omniscript RT kit (Qiagen). Real-time RT-PCRs were carried out using Dynamo qPCR chemistry (Finnzymes, Espoo, Finland), with pre-designed gene-specific primers obtained from Qiagen.

3.5. Histological stains, [^{35}S]sulfate labeling and in situ hybridization

For quantification of ECM production, cells were grown in the presence of 10 μCi/ml of [^{35}S]sulfate (Perkin Elmer, Boston, MA) for 72 h, and the incorporated radioactivity was determined by liquid scintillation. For alcian blue and alizarin red staining, micromass cultures were fixed in paraformaldehyde, stained with 0.5% alcian blue in HCl or 2% alizarin red in distilled water overnight, and photographed with a Leica S6D microscope. Tibias were fixed in paraformaldehyde, decalcified in EDTA, embedded in paraffin and sectioned at the thickness of 5 μm. Alternative slides were stained by hematoxylin–eosin for morphological analysis. For in situ hybridization, plasmid Col10a1 (IMAGp998B1114092Q, Biovalley) was linearized by PCR reaction with M13 primers. Sense and antisence DIG labeled riboprobes were produced by SP6 and T7 RNA polymerase, respectively. Hybridization was performed at 60 °C overnight. Sense DIG labeled probe was used as negative control. Slides were counterstained with eosin.

Supplementary data to this article can be found online at http://dx.doi.org/10.1016/j.bbadis.2014.12.020.

Acknowledgment

We thank M. Schibler for the help with confocal microscopy, J. Martin for the critical reading of the manuscript, P. Mekikian for the excellent technical assistance and J. Medalova for the assistance with manuscript preparation. This work was supported by the Ministry of Education, Youth and Sports of the Czech Republic (KONTAKT LH12004, CZ.1.07/2.3.00/30.0053), Czech Science Foundation (204/09/0498, P302/12/J059, GBP302/12/G157, 14-31540S), Grant Agency of Masaryk University (0071-2013, MUNI/A/0793/2012), European Regional Development Fund (FNUSA-ICRC No.CZ.1.05/1.1.00/02.0123), and the European Union (ICRC-ERA-HumanBridge No.316345).

References

[1] S. Provot, E. Schipani, Molecular mechanisms of endochondral bone development, Biochem. Biophys. Res. Commun. 328 (3) (2005) 658–665.
[2] J.S. Colvin, B.A. Bohne, G.W. Harding, D.G. McEwen, D.M. Ornitz, Skeletal overgrowth and deafness in mice lacking fibroblast growth factor receptor 3, Nat. Genet. 12 (4) (1996) 390–397.
[3] D.K. Waller, A. Correa, T.M. Vo, Y. Wang, C. Hobbs, et al., The population-based prevalence of achondroplasia and thanatophoric dysplasia in selected regions of the US, Am. J. Med. Genet. A 146A (2008) 2385–2389.
[4] S. Foldynova-Trantirkova, W.R. Wilcox, Krejci, Sixteen years and counting: the current understanding of fibroblast growth factor receptor 3 (FGFR3) signaling in skeletal dysplasias, Hum. Mutat. 33 (1) (2012) 29–41.
[5] H.M. Kronenberg, PTHrP and skeletal development, Ann. NY Acad. Sci. 1068 (2006) 1–13.
[6] M.C. Naski, J.S. Colvin, J.D. Coffin, D.M. Ornitz, Repression of hedgehog signaling and BMP4 expression in growth plate cartilage by fibroblast growth factor receptor 3, Development 125 (1998) 4977–4988.
[7] L. Chen, R. Adar, X. Yang, E.O. Monsonego, C. Li, et al., Gly369Cys mutation in mouse FGFR3 causes achondroplasia by affecting both chondrogenesis and osteogenesis, J. Clin. Invest. 104 (11) (1999) 1517–1525.
[8] C. Li, L. Chen, T. Iwata, M. Kitagawa, X.Y. Fu, C.X. Deng, A Lys644Glu substitution in fibroblast growth factor receptor 3 (FGFR3) causes dwarfism in mice by activation of STATs and ink4 cell cycle inhibitors, Hum. Mol. Genet. 8 (1999) 35–44.

[9] Y. Yamanaka, H. Tanaka, M. Koike, R. Nishimura, Y. Seino, PTHrP rescues ATDC5 cells from apoptosis induced by FGF receptor 3 mutation, J. Bone Miner. Res. 18 (2003) 1395–1403.
[10] P. Krejci, A. Aklian, M. Kaucka, E. Sevcikova, J. Prochazkova, et al., Receptor tyrosine kinases activate canonical WNT/beta-catenin signaling via MAP kinase/LRP6 pathway and direct beta-catenin phosphorylation, PLoS ONE 7 (4) (2012) e35826.
[11] K. Tamai, X. Zeng, C. Liu, X. Zhang, Y. Harada, et al., A mechanism for Wnt coreceptor activation, Mol. Cell 13 (1) (2004) 149–156.
[12] A.C. Andrade, O. Nilsson, K.M. Barnes, J. Baron, Wnt gene expression in the postnatal growth plate: regulation with chondrocyte differentiation, Bone 40 (5) (2007) 1361–1369.
[13] Y.F. Dong, Y. Soung do, E.M. Schwarz, R.J. O'Keefe, H. Drissi, Wnt induction of chondrocyte hypertrophy through the runx2 transcription factor, J. Cell. Physiol. 208 (1) (2006) 77–86.
[14] X. Guo, K.K. Mak, M.M. Taketo, Y. Yang, The Wnt/beta-catenin pathway interacts differentially with PTHrP signaling to control chondrocyte hypertrophy and final maturation, PLoS ONE 4 (6) (2009) e6067.
[15] K. Mukhopadhyay, V. Lefebvre, G. Zhou, S. Garofalo, J.H. Kimura, B. de Crombrugghe, Use of a new rat chondrosarcoma cell line to delineate a 119-base pair chondrocyte-specific enhancer element and to define active promoter segments in the mouse pro-alpha 1(II) collagen gene, J. Biol. Chem. 270 (46) (1995) 27711–27719.
[16] P. Krejci, V. Bryja, J. Pachernik, A. Hampl, R. Pogue, et al., FGF2 inhibits proliferation and alters the cartilage-like phenotype of RCS cells, Exp. Cell Res. 297 (1) (2004) 152–164.
[17] O. Rozenblatt-Rosen, E. Mosonego-Ornan, E. Sadot, L. Madar-Shapiro, Y. Sheinin, et al., Induction of chondrocyte growth arrest by FGF: transcriptional and cytoskeletal alterations, J. Cell Sci. 115 (2002) 553–562.
[18] K. Daniels, R. Reiter, M. Solursh, Micromass cultures of limb and other mesenchyme, Methods Cell Biol. 51 (1996) 237–247.
[19] S.W. Gay, R.A. Kosher, Uniform cartilage differentiation in micromass cultures prepared from a relatively homogeneous population of chondrogenic progenitor cells of the chick limb bud: effect of prostaglandins, J. Exp. Zool. 232 (2) (1984) 317–326.
[20] C. Niehrs, J. Shen, Regulation of Lrp6 phosphorylation, Cell. Mol. Life Sci. 67 (2010) 2551–2562.
[21] J. Wolf, T.R. Palmby, J. Gavard, B.O. Williams, J.S. Gutkind, Multiple PPPS/TP motifs act in a combinatorial fashion to transduce Wnt signaling through LRP6, FEBS Lett. 582 (2008) 255–261.
[22] I. Cervenka, J. Wolf, J. Masek, P. Krejci, W.R. Wilcox, et al., Mitogen-activated protein kinases promote WNT/beta-catenin signaling via phosphorylation of LRP6, Mol. Cell. Biol. 31 (1) (2011) 179–189.
[23] C.A. de Frutos, S. Vega, M. Manzanares, J.M. Flores, H. Huertas, et al., Snail1 is a transcriptional effector of FGFR3 signaling during chondrogenesis and achondroplasias, Dev. Cell 13 (6) (2007) 872–883.
[24] V. Lefebvre, W. Huang, V.R. Harley, P.N. Goodfellow, B. de Crombrugghe, SOX9 is a potent activator of the chondrocyte-specific enhancer of the pro alpha1(II) collagen gene, Mol. Cell. Biol. 4 (1997) 2336–2346.
[25] R. Pogue, K. Lyons, BMP signaling in the cartilage growth plate, Curr. Top. Dev. Biol. 76 (2006) 1–48.
[26] A. Vortkamp, K. Lee, B. Lanske, G.V. Segre, H.M. Kronenberg, C.J. Tabin, Regulation of rate of cartilage differentiation by Indian hedgehog and PTH-related protein, Science 273 (5275) (1996) 613–622.
[27] S. Wu, A. Morrison, H. Sun, F. De Luca, Nuclear factor-kappaB (NF-kappaB) p65 interacts with Stat5b in growth plate chondrocytes and mediates the effects of growth hormone on chondrogenesis and on the expression of insulin-like growth factor-1 and bone morphogenetic protein-2, J. Biol. Chem. 286 (28) (2011) 24726–24734.
[28] M.A. Mello, R.S. Tuan, High density micromass cultures of embryonic limb bud mesenchymal cells: an in vitro model of endochondral skeletal development, In Vitro Cell. Dev. Biol. Anim. 35 (1999) 262–269.
[29] M. Sahni, D.C. Ambrosetti, A. Mansukhani, R. Gertner, D. Levy, C. Basilico, FGF signaling inhibits chondrocyte proliferation and regulates bone development through the STAT-1 pathway, Genes Dev. 13 (11) (1999) 1361–1366.
[30] P. Krejci, B. Masri, V. Fontaine, P.B. Mekikian, M. Weis, et al., Interaction of fibroblast growth factor and C-natriuretic peptide signaling in regulation of chondrocyte proliferation and extracellular matrix homeostasis, J. Cell Sci. 118 (Pt 21) (2005) 5089–5100.
[31] P. Krejci, J. Prochazkova, J. Smutny, K. Chlebova, P. Lin, et al., FGFR3 signaling induces a reversible senescence phenotype in chondrocytes similar to oncogene-induced premature senescence, Bone 47 (1) (2010) 102–110.
[32] A.M. Malfait, R.Q. Liu, K. Ijiri, S. Komiya, M.D. Tortorella, Inhibition of ADAM-TS4 and ADAM-TS5 prevents aggrecan degradation in osteoarthritic cartilage, J. Biol. Chem. 277 (25) (2002) 22201–22208.
[33] J.C. Rodríguez-Manzaneque, J. Westling, S.N. Thai, A. Luque, V. Knauper, et al., ADAMTS1 cleaves aggrecan at multiple sites and is differentially inhibited by metalloproteinase inhibitors, Biochem. Biophys. Res. Commun. 293 (1) (2002) 501–508.
[34] B. Caterson, C.R. Flannery, C.E. Hughes, C.B. Little, Mechanisms involved in cartilage proteoglycan catabolism, Matrix Biol. 19 (4) (2000) 333–344.
[35] M. Maeda, H. Hasegawa, T. Hyodo, S. Ito, E. Asano, et al., ARHGAP18, a GTPase-activating protein for RhoA, controls cell shape, spreading, and motility, Mol. Biol. Cell 22 (20) (2011) 3840–3852.
[36] Y.A. Tang, W.L. Wen, J.W. Chang, T.T. Wei, Y.H. Tan, et al., A novel histone deacetylase inhibitor exhibits antitumor activity via apoptosis induction, F-actin disruption and gene acetylation in lung cancer, PLoS ONE 5 (9) (2010) e12417.
[37] K. Wong, X.R. Ren, Y.Z. Huang, Y. Xie, et al., Signal transduction in neuronal migration: roles of GTPase activating proteins and the small GTPase Cdc42 in the Slit-Robo pathway, Cell 107 (2) (2001) 209–221.
[38] J. Tcherkezian, I. Triki, R. Stenne, E.I. Danek, N. Lamarche-Vane, The human orthologue of CdGAP is a phosphoprotein and a GTPase-activating protein for Cdc42 and Rac1 but not RhoA, Biol. Cell. 98 (8) (2006) 445–456.
[39] K. Kaibuchi, S. Kuroda, M. Amano, Regulation of the cytoskeleton and cell adhesion by the Rho family GTPases in mammalian cells, Annu. Rev. Biochem. 68 (1999) 459–486.
[40] S. Narumiya, The small GTPase Rho: cellular functions and signal transduction, J. Biochem. 120 (2) (1996) 215–228.
[41] S.M. Schoenwaelder, K. Burridge, Bidirectional signaling between the cytoskeleton and integrins, Curr. Opin. Cell Biol. 11 (2) (1999) 274–286.
[42] K. Nakamura, J. Nishimura, K. Hirano, S. Ibayashi, M. Fujishima, H. Kanaide, Hydroxyfasudil, an active metabolite of fasudil hydrochloride, relaxes the rabbit basilar artery by disinhibition of myosin light chain phosphatase, J. Cereb. Blood Flow Metab. 21 (7) (2001) 876–885.
[43] M. Uehata, T. Ishizaki, H. Satoh, T. Ono, T. Kawahara, et al., Calcium sensitization of smooth muscle mediated by a Rho-associated protein kinase in hypertension, Nature 389 (6654) (1997) 990–994.
[44] M. Diez, M.M. Musri, E. Ferrer, J.A. Barbera, V.I. Peinado, Endothelial progenitor cells undergo an endothelial-to-mesenchymal transition-like process mediated by TGFbetaRI, Cardiovasc. Res. 88 (3) (2010) 502–511.
[45] Y. Kanazawa, Y. Doi, H. Kudo, S. Fujimoto, Immunolocalization of fibronectin and its receptors integrin alpha 3 and alpha 5 subunits in the rat limb development, J. Electron. Microsc. (Tokyo) 47 (1) (1998) 87–92.
[46] A. Mirza, L. Foster, H. Valentine, I. Welch, C.M. West, S. Pritchard, Investigation of the epithelial to mesenchymal transition markers S100A4, vimentin and Snail1 in gastroesophageal junction tumors, Dis. Esophagus (2012), http://dx.doi.org/10.1111/j.1442-2050.2012.01435.x.
[47] B. Sagi, P. Maraghechi, V.S. Urban, B. Hegyi, A. Szigeti, et al., Positional identity of murine mesenchymal stem cells resident in different organs is determined in the postsegmentation mesoderm, Stem Cells Dev. 21 (5) (2012) 814–828.
[48] L. Dailey, E. Laplantine, R. Priore, C. Basilico, A network of transcriptional and signaling events is activated by FGF to induce chondrocyte growth arrest and differentiation, J. Cell Biol. 161 (6) (2003) 1053–1066.
[49] W.A. Horton, O.J. Hood, M.A. Machado, S. Ahmed, E.S. Griffey, Abnormal ossification in thanatophoric dysplasia, Bone 9 (1) (1988) 53–61.
[50] L. Chen, C. Li, W. Qiao, X. Xu, C. Deng, A Ser(365)− > Cys mutation of fibroblast growth factor receptor 3 in mouse downregulates Ihh/PTHrP signals and causes severe achondroplasia, Hum. Mol. Genet. 10 (2001) 457–465.
[51] A. Ornoy, G.E. Adomian, D.J. Eteson, R.E. Burgeson, D.L. Rimoin, The role of mesenchyme-like tissue in the pathogenesis of thanatophoric dysplasia, Am. J. Med. Genet. 21 (4) (1985) 613–630.
[52] S. Weizmann, A. Tong, A. Reich, O. Genina, A. Yayon, E. Monsonego-Ornan, FGF upregulates osteopontin in epiphyseal growth plate chondrocytes: implications for endochondral ossification, Matrix Biol. 24 (8) (2005) 520–529.
[53] D. Kumar, A.B. Lassar, The transcriptional activity of Sox9 in chondrocytes is regulated by RhoA signaling and actin polymerization, Mol. Cell. Biol. 29 (15) (2009) 4262–4273.
[54] G. Wang, A. Woods, S. Sabari, L. Pagnotta, L.A. Stanton, F. Beier, RhoA/ROCK signaling suppresses hypertrophic chondrocyte differentiation, J. Biol. Chem. 279 (13) (2004) 13205–13214.
[55] T.P. Hill, D. Spater, M.M. Taketo, W. Birchmeier, C. Hartmann, Canonical Wnt/beta-catenin signaling prevents osteoblasts from differentiating into chondrocytes, Dev. Cell 8 (5) (2005) 727–738.
[56] B. Ning, P. Wang, X. Pei, Y. Kang, J. Song, et al., Dual function of beta-catenin in articular cartilage growth and degeneration at different stages of postnatal cartilage development, Int. Orthop. 36 (3) (2012) 655–664.
[57] Y. Tamamura, T. Otani, N. Kanatani, E. Koyama, J. Kitagaki, et al., Developmental regulation of Wnt/beta-catenin signals is required for growth plate assembly, cartilage integrity, and endochondral ossification, J. Biol. Chem. 280 (19) (2005) 19185–19195.
[58] L. Zawel, J.L. Dai, P. Buckhaults, S. Zhou, K.W. Kinzler, et al., Human Smad3 and Smad4 are sequence-specific transcription activators, Mol. Cell 1 (4) (1998) 611–617.
[59] K. Horiguchi, T. Shirakihara, A. Nakano, T. Imamura, K. Miyazono, M. Saitoh, Role of Ras signaling in the induction of snail by transforming growth factor-beta, J. Biol. Chem. 284 (1) (2009) 245–253.
[60] V. Lefebvre, G. Zhou, K. Mukhopadhyay, C.N. Smith, Z. Zhang, et al., An 18-base-pair sequence in the mouse proalpha1(II) collagen gene is sufficient for expression in cartilage and binds nuclear proteins that are selectively expressed in chondrocytes, Mol. Cell. Biol. 16 (8) (1996) 4512–4523.
[61] H. Sasaki, C. Hui, M. Nakafuku, H. Kondoh, A binding site for Gli proteins is essential for HNF-3beta floor plate enhancer activity in transgenics and can respond to Shh in vitro, Development 124 (7) (1997) 1313–1322.